Composite Materials and Structural Glass: Adhesion Phenomena

E. Speranzini*

Department of Engineering, University of Perugia, via Duranti n. 93, 06125 Perugia, Italy

Abstract: This study aims to investigate the adhesion phenomena between glass and composite materials, which - if they work in synergy – can increase the performance of glass structures, as regard both structural elements and the manufacture of joints. The experimental programme consisted of shear traction tests on all samples: glass-glass single-lap shear adhesion, glass-GFRP double-lap shear adhesion and glass-SRP shear adhesion. Different types of adhesive and various interface geometries were also tested to evaluate the ultimate force and identify fracture patterns with different bonding lengths. It was possible to identify the effective bonding length for each type of resin used to prepare test samples, by taking fracture load and average peel stress into account. Bonding length variations were also recorded. This enabled the values of bonding length to be verified analytically. Based on experimental results, a formula for the evaluation of delamination resistance and the optimal bonding length is proposed.

Keywords: GFRP, SRP, Adhesion, Structural glass.

1. INTRODUCTION

Designing with glass is challenging because of its fragility that produces sudden failure without any form of alarm or forewarning [1]. Glass is an elastic brittle material until failure, and the need for a post-critical phase has been the scope a number of studies developed in the last few years [2-4]. Several ways of improving glass strength, by reinforcing glass elements by means of additive materials, have been the object of various researches. Hybrid beams have been obtained by coupling glass with glass or carbon fibre strips [5], or CFRP rebar [6], or steel band [7], or steel profile [8-11], or GFRP pultruded profiles [12, 13]. In addition, various investigations about the behaviour of adhesives have been performed, in order to determine the material properties of bonding, to ensure a better design of the elements [14, 15].

This study aims to investigate the adhesion phenomena between glass and composite materials. The experimental programme consisted of shear traction tests on all samples: glass-glass single-lap shear adhesion, glass-GFRP double-lap shear adhesion and glass-SRP shear adhesion. Different types of adhesive and various interface geometries were also tested [16]. The experiment carried out on samples enabled to evaluate the ultimate force and identify the fracture patterns, when bonding length was varied. In the case of adhesion with composite materials, it was possible to identify the effective bonding length for each type of resin used to prepare test samples, by taking fracture load and average peel stress into account. Length variations, applied to the joint in glass-SRP samples, were also recorded. This enabled to verify bonding length values analytically.

Substantiated theories were used to study the behaviour of epoxy resins in composite bonding and making [17, 18]. The theoretical results obtained from these theories proved to concur with experimentally measured values, and validated the suitability of the theory for epoxy resins.

2. MATERIAL PROPERTIES

Tested samples were made of glass bonded by epoxy resins or bonded with glass and steel fibre using resins. All test samples were produced using 8 mm-thick sheets of annealed glass, specially cut in various sizes according to the different types of tests. The float glass used according to the EN 572 standard has the following mechanical properties: density 2500 kg/m3, Young's modulus 70000 MPa, Poisson's ratio 0.2 and flexural tensile stress 45 MPa.

Due to the nature of the glass surface, the resin used to impregnate the fibres also acts as an adhesive: for this reason, it must not only have good impregnability, but also suitable adhesive requisites for the material to be reinforced.

Two different matrixes were used for glass adhesion tests, with a single-lap joint. The two adhesives, both bi-component epoxy resins, show similar mechanical characteristics, but differ in colour and viscosity. One is a very fluid, transparent resin; the other is a pasty, light grey, thixotropic resin (resins 1 and 2 in Table **1**). They are both structural resins, commonly used for FRP reinforcements.

*Address correspondence to this author at the Department of Engineering, University of Perugia, via Duranti n. 93, 06125 Perugia, Italy;
Tel: +393683911688; E-mail: emanuela.speranzini@unipg.it

E-ISSN: 2409-9848/18

Three resins were tested on samples reinforced with GFRP and SRP: the two resins mentioned above, and a third white, pasty, bi-component epoxy resin (resin 3 in Table **1**). From an aesthetical viewpoint, resin 1 is the most suitable because it is completely transparent and does not change colour over time. The other two resins are not only coloured, but also denser than the preceding resin.

The glass fibres used for the composite consist of 320 g/m^2 unidirectional fabric (tensile strength 2900 MPa, Young's modulus 71 GPa, tensile elongation 4.5 ± 0.5%). They are white and, contrary to glass, have a high tensile strength due to the processes they have undergone. The UHTSS steel fibres used to make the composite consist of cords placed longitudinally to form a unidirectional fabric, weighing 1500 g/m^2 (tensile strength 2950 MPa, Young's modulus 206 GPa, tensile elongation 2.3%). The steel fibres are gold-coloured, with a high tensile strength and, contrary to other fibres; they also have a reasonable shear strength. They are combined with epoxy resin to obtain SRP (Steel Reinforced Polymer).

3. METHODS AND RESULTS

3.1. Experimental Tests - Glass Adhesion Tests with a Single-Lap Joint

Samples were made of two small, annealed glass sheets, measuring 8x50x80 mm. They were stacked and glued with different types of resins composing a surface of 20 mm x50 mm. Bonding was guaranteed by a small layer of adhesive between glass sheets, and samples were tested as soon as resins were fully hardened. Using appropriate metal shearing elements, able to distribute the load on the axis of the element (coplanar with the bonding surface), the elements underwent a traction test, anchoring the clamps of metallic supports to the tensile test machine (Figure **1**).

Tests were performed at the same displacement rate (2 mm/min), in compliance with the instructions in EN 1465:2009 "Determination of tensile lap-shear strength bonded assemblies".

Table **2** shows the maximum tensile stress and shear stress, together with the mean value of shear stress that represents the adhesion stress τ_m. The value of the maximum tangential stresses on the

Table 1: Physical and Mechanical Properties of Resins (from Manufacturer)

	Resin 1	Resin 2	Resin 3
Density [g/cm^3]	1.08	1.9	1.5
Consistence	Liquid	thixotropic	mellow
Colour	transparent	Light grey	white
Pot-Life a 20°C (mass of 500 g) [min]	20	20	25
Time of complete gardening at 20°C [days]	7	7	7
Compression strength [Mpa]	50	56	95
Flexural strength [Mpa]	30	16	30
Young's modulus [Mpa]	1760	1780	2200

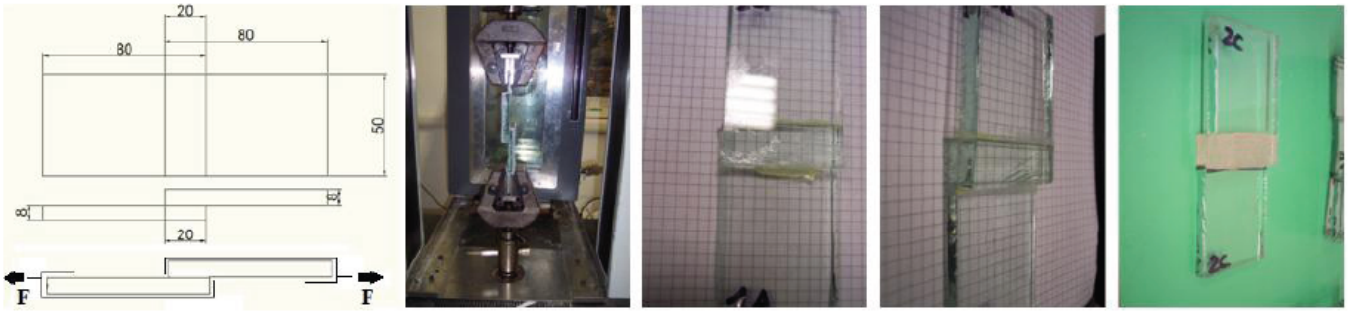

Figure 1: Sample size, test setup and samples with different resins.

average plane of the adhesive τ_{max}, as well as the normal stress σ_{max}, were obtained according to the "beam on elastic soil" analytical model, originally suggested by Goland and Reissner [19]. This is based on the hypothesis that deformations in the adherends are determined by adherend flexure, since the orthogonal deformation to the adherend plane and the shear deformation in the adherends, compared with those of the adhesive, can be considered as negligible. Moreover, the adhesive layer can be configured as a system of springs placed between the two adherends in normal and tangential direction (Figure **2**).

The following equations were used to calculate the trend of the stress and strain state along the bond surface, corresponding to the failure load recorded during experimental tests.

$$\tau(x)=\frac{p\cdot t}{4\cdot L_a}\left[\frac{\beta\cdot L_a}{2\cdot t}(1+3k)\cdot\frac{\cosh\frac{\beta(2x-L_a)}{2\cdot t}}{\sinh\frac{\beta L_a}{2\cdot t}}+3\cdot(1-k)\right], \quad (1)$$

$$\sigma(x)=\frac{8\cdot p\cdot t^2}{\Delta\cdot L_a}\left[\begin{matrix}\left(R_2\lambda^2\frac{k}{2}+\lambda\cdot k'\cdot\cosh\lambda\cos\lambda\right)\cosh\lambda'\cos\lambda'+\\+\left(R_1\lambda^2\frac{k}{2}+\lambda\cdot k'\cdot\sinh\lambda\sin\lambda\right)\sinh\lambda'\sin\lambda'\end{matrix}\right], \quad (2)$$

where:

$$p=\frac{F}{w\cdot L_a}, \quad (3)$$

$$\beta=\sqrt{\frac{4\cdot E_a\cdot t}{(1+\nu_a)\cdot t_a\cdot E}}, \quad (4)$$

$$\lambda=\frac{L_a}{2t}\left(\frac{6\cdot E_a\cdot t}{t_a\cdot E}\right)^{1/4}, \quad (5)$$

$$\lambda'=\lambda\frac{2x-L_a}{L_a}, \quad (6)$$

$$\Delta=\sinh(2\lambda)+\sin(2\lambda), \quad (7)$$

$$k=\left[1+2\sqrt{2\cdot\tanh\left(\frac{L_a}{2\cdot t}\right)\sqrt{\frac{3\cdot p\cdot(1-\nu^2)}{2\cdot E}}}\right]^{-1}, \quad (8)$$

$$k'=\frac{k\cdot L_a}{2\cdot t}\sqrt{\frac{3\cdot p\cdot(1-\nu^2)}{E}}, \quad (9)$$

$$R_1=\sinh\lambda\cdot\cos\lambda+\cosh\lambda\cdot\sin\lambda, \quad (10)$$

$$R_2=\sinh\lambda\cdot\cos\lambda-\cosh\lambda\cdot\sin\lambda, \quad (11)$$

where *x* is the longitudinal coordinate starting from the edge of the adhesive. In numerical terms, it is useful to prove that the observed values of maximum and minimum effort are subject to change as a function of the models used and reference assumptions. The model proposed here has been validated numerically and is similar to that used by some international design codes.

Symbols have the following meanings:

τ(x)= is the shear stress as a function of the position along the length L_a;

σ(x)= is the detachment stress as a function of the position along the length L_a;

F= is the failure load;

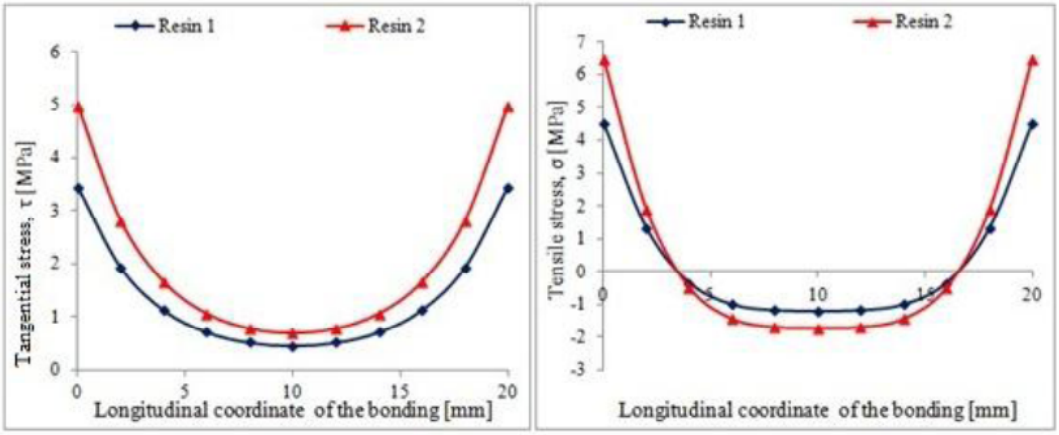

Figure 2: Tangential and tensile stress distributions along the bonding of the glass-glass single-lap shear sample.

t= is the thickness of the elements;

E= is the Young modulus of the material of support;

v= is the Poisson ratio of the material of support;

t_a= is the thickness of the adhesive;

E_a= is the Young modulus of the adhesive;

v_a= is the Poisson ratio of the adhesive;

L_a= is the length of the bonding;

w= is the width of the bonding.

A visual inspection of the samples after failure provides information about the typology of the rupture of adhesives. Both resins showed an adhesive fracture, *i.e*. in the interface between the adhesive and the support, which occurs when the interface resistance (adhesive strength) is less than the cohesive strength of the support (Table **2**). Following peeling, fracture surfaces are perfectly smooth: the glass is intact, clean and without any abrasions, just as it was before the resin was applied.

3.2. Experimental Tests - Glass and Composite Shear Adhesion Tests

Two sets of samples were made as regards the adhesion between glass and GFRP, and two different sets of samples were prepared with glass and SRP (Figure **3**).

3.2.1. Glass-GFRP

The first glass-GFRP samples were obtained, gluing the fibre (prepared using resin 1 for each bonding length measuring 50 mm, 100 mm and 150 mm and width of 20 mm) onto the two external surfaces of a glass sheet, producing a circle so that they could be hooked to the loading system. The second samples were made by laying a fibre strip (width 20 mm, length varying between 50 and 200 mm) between two glass sheets. The fibre was fastened to the outgoing end of the sheet, so that it could be hooked to the traction system. With this setup, 5 samples were prepared using resin 2 for the bonding length of 200 mm, and 5 samples using resin 3 for the bonding lengths of 100, 150, 200 and 300 mm (Table **3**).

From an analysis of the results, the ultimate value of the force that the GFRP reinforcement can resist before delamination takes over depends on the length of the bonded area. This value increases with the bonding length, until it reaches a maximum, corresponding to a well-defined length. Increasing the bonded area further does not result in an increase in the force transmitted. Thus, it is possible to determine the bonding length that guarantees transmission of the maximum adhesion stress and allows reaching the

Table 2: Mean Values of Tensile-Shear Tests on Glass-Glass Samples

	Experimental values							Theoretical Values	
	Samples number	**Width [mm]**	**Bonding Length [mm]**	**Force [N]**	**τ_m [Mpa]**	**Bond Elongation [mm]**	**Maximum Strain [%]**	**τ_{max} [MPa]**	**σ_{max} [MPa]**
Resin 1	10	50.46	19.71	2516.31	2.53	2.04	1.46	2.86	3.76
Resin 2	5	51.47	20.35	5054.72	4.83	1.88	1.35	5.66	7.33

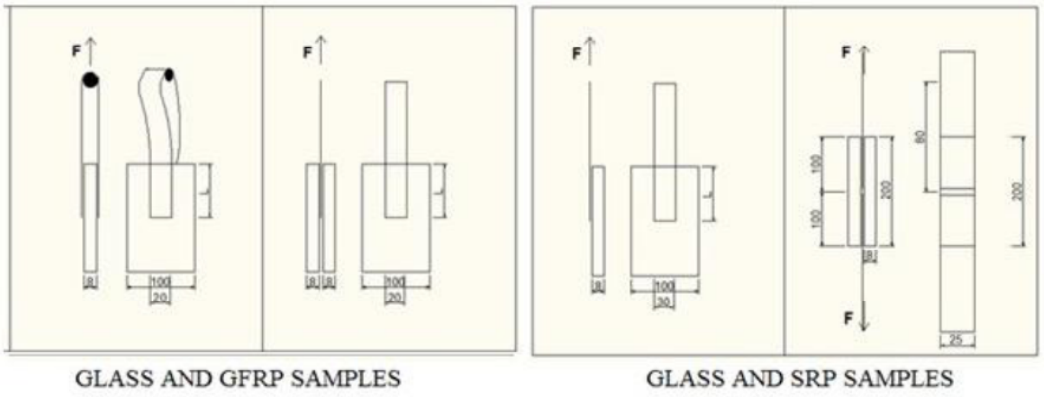

Figure 3: Size of glass-GFRP and glass-SRP samples.

Table 3: Mean Results of Adhesion Tests on the GFRP for Resins 1, 2 and 3

	Samples number	Width [mm]	Bonding length [mm]	Force [N]	τ_m [Mpa]	Type of failure
	10	20	50	6.97	6.97	adhesive
Resin 1	10	20	100	8.01	4	traction of the fibre - 80%
	10	20	150	9.82	3.27	traction of the fibre - 100%
Resin 2	5	20	200	5.55	1.39	adhesive
	5	20	100	3.47	1.74	adhesive
	5	20	150	4.96	1.65	adhesive
Resin 3	5	20	200	5.31	1.33	adhesive
	5	20	250	6.42	1.28	traction of the fibre - 60%
	5	20	300	7.44	1.24	traction of the fibre - 100%

fibre tensile strength before delamination. Based on investigation results, the aforementioned bonding length can be calculated at: 120 mm for resin 1, 200 mm for resin 2, 280 mm for resin 3.

3.2.2. Glass-SRP

Shear traction tests on the adhesion between glass and steel fibre used samples made of two types of joints: single-lap shear and double-lap shear.

Samples with a *single-lap shear joint* were made with glass glued to 30-mm-wide steel fibre strips, varying between 50 and 200 mm in length. Five samples measuring 50, 100, 150 and 200 mm in length were prepared for each one of resins 1 and 3 in order to apply the fibre. The tests results of these samples are shown in Table **4** where it can be observed that resin1 is able to transfer a higher load compared to resin 3. As regards resin 1, a high increase of the adhesion load in the range 50-100 mm bond length was obtained. At the contrary, the transferred load was almost constant in the range 150-200 mm after which its increments were irrelevant. Therefore, 200 mm can be considered a good bond length for resin 1.

The samples with a *double-lap shear joint* were made gluing two steel fibre strips 25 mm in width and 100 mm in length between two sheets of glass. Five samples were prepared for each one of resins 1 and 2 used to glue the fibre. The results of these tests are summarised in Table **5** where it is shown that Resin 1 is the most suitable. In fact, its high fluidity allows a perfect impregnation of the fiber and a reliable bonding to glass making a good union.

3.3. Delamination and Optimal Length

The delamination phenomenon is one of the two failure causes for the samples tested, which are the debonding of the composite and the failure of the FRP because of tensile strength achievement [20]. Both these conditions cause system failure, but the former not always guarantees a complete transfer of stresses

Table 4: Mean Results of Adhesion Tests on Glass-SRP Single-lap Shear Samples

	Samples Number	Width [mm]	Bonding Length [mm]	Force [N]	τ_m [Mpa]	Type of Failure
Resin 1	5	30	50	4717.40	3.14	adhesive
	5	30	100	6578.90	2.19	adhesive
	5	30	150	6984.70	1.55	adhesive
	5	30	200	7004.90	1.17	adhesive
Resin 3	5	30	50	1589.86	1.06	adhesive
	5	30	100	2333.10	0.78	adhesive
	5	30	150	3859.17	0.86	adhesive
	5	30	200	5168.53	0.86	adhesive

Table 5: Mean Results of Adhesion Tests on Glass-SRP Double-lap Shear Samples

	Samples Number	Width [mm]	Bonding Length [mm]	Force [N]	τ_m [MPa]	Bond Elongation at the Maximum Load [mm]	Bond Elongation at Failure [mm]	Type of Failure
Resin 1	5	25	100	7271.90	1.44	6.35	6.35	adhesive
Resin 2	5	25	100	3425.41	0.69	8.08	8.74	adhesive

between the glass and FRP. The system can transmit the maximum amount of stresses only if the adhesion length of the composite is adequate. On the contrary, if the adhesion surface is smaller (*i.e*. the adhesion length is shorter than a certain measure), the system cannot transmit the maximum stress it can bear; in this case, failure happened prematurely, making the joint design inadequate.

If the adhesion length is longer that an adequate amount permitting the maximum stress to be transferred, there is no advantage with respect to the stresses transmitted.

This study evaluated the resistance to detachment of the reinforcement. When reinforcing glass elements using composite materials, the role of adhesion between the support and composite is of great importance since the failure mechanism for detachment from the underlying material is fragile. According to the criterion of strength hierarchy, such crisis mechanism must not precede the collapse of other parts of the structure (*i.e*. collapse for bending or shear).

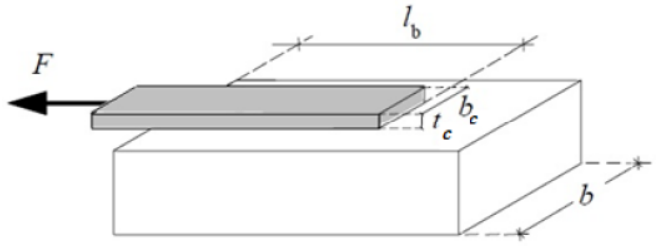

Figure 4: Layout of the adhesion test.

Referring to a typical adhesion test, such as that schematically represented in Figure **4**, the ultimate value of the force supported by the FRP, before detaching from the support, depends on the length, l_b, of the bonded area. This value increases with l_b up to a maximum corresponding to a well-defined length, l_e: further increases of the bonded area do not lead to increases in the strength transmitted. Length is defined as the optimal bonding length and corresponds to the minimum anchorage length, which ensures the transmission of the maximum adhesion effort. The values t_c, b_c and b represent the thickness and width of the reinforcement respectively and the width of the support.

The relation (12) proposes the evaluation of delamination resistance, f_{fd}, as a function of the modulus of elasticity of the composite, E_c, of the thickness of the FRP, t_c, and of a value called specific energy of fracture Γ_{Fk}, in the hypothesis of a linear behaviour of adhesives extending the elastic field very close to the fragile failure point:

$$f_{fd} = \sqrt{\frac{2 \cdot E_c \cdot \Gamma_{Fk}}{t_c}}. \quad (12)$$

E_c can be calculated using the rule of mixture, in the case of unidirectional composites.

The specific energy of fracture (13) depends on tensile strength, $f_{mat,t}$, compressive strength, $f_{mat,c}$, of the matrix and a coefficient, c, evaluated on the basis of experimental considerations:

$$\Gamma_{Fk} = c \cdot \sqrt{f_{mat,t} \cdot f_{mat,c}}. \quad (13)$$

The value attributed to the parameter “c” is 1.7·10-7 (dimensionless).

The length l_e, derived from experimental evidence, ensures total transfer of stresses between the composite and the glass across the adhesion area:

$$l_e = 10 \cdot \frac{f_{mat,t}}{f_{mat,c}} \sqrt{\frac{E_c \cdot t_c^2}{2 \cdot f_{mat,t}}}. \quad (14)$$

These formulae were used to calculated the values of the delamination resistance and the optimal adhesion length in the case of composites in steel-fiber and glass-fiber. The theoretical values obtained (Table **6**) are in line with experimental results and in general are greater so these values are on the safe side.

Table 6: Values of Delamination Resistance and Optimal Adhesion Length Obtained with the Model

TEST N°	Type of resin	Type of fibre	f_{fd} [MPa]	l_e [mm]	Experimental Values of l_e
Test 1	Resin 1	UHTSS fibre	0.98	231.78	> 100
Test 2	Resin 2	UHTSS fibre	0.83	139.93	> 100
Test 3	Resin 3	Glass fibre	1.18	247.63	280
Test 4	Resin 1	Glass fibre	3.06	95.54	120
Test 5	Resin 2	Glass fibre	1.43	187.25	> 200
Test 6	Resin 1	UHTSS fibre	0.98	231.78	200
Test 7	Resin 3	UHTSS fibre	0.80	156.60	150

DISCUSSION AND CONCLUSIONS

This experiment made it possible to study the adhesion phenomena between composite materials and glass in order to assess the bonding adequacy of the two materials. This phenomenon is especially important in composite glass beams, where the tensile resistant materials considerably increase the strength of glass structural elements and improve their behaviour in post-fracture phase. Investigation looked into glass-glass, glass-GFRP and glass-SRP adhesion and checks on three different resins used for the impregnation of the fibre and for the gluing of the glass.

Resin 1 is the most suitable for glass structures, because it is aesthetically attractive and mechanically effective. The high fluidity of this resin makes it particularly suitable for bonding glass to fibres, as it can perfectly impregnate both glass and steel fibres. However, in samples where fibre impregnation is less important and resin is compressed between two glass sheets, results are more satisfactory using resin 2. In this case, resin 1 appears to give a poorer grip than resin 2, as it is also influenced by the scant amount of resin remaining between the two glass sheets, due to its fluidity. A better result can be achieved, if a thicker resin layer is obtained by placing it inside a mould.

The adhesion tests allowed evaluating the type of failure and the mean adhesion stress for each test category to understand the adequate adhesion length. Resin1 is the best in the GFRP-glass adhesion and SRP-glass adhesion because requires a smaller bond length to give the adequate adhesion so that the composites reach its maximum resistance. Its viscous liquid consistency allows perfectly impregnating the fibres and obtaining a reliable glass-composite union.

Generally speaking, in terms of design philosophy the constituent materials should be able to transfer the maximum stresses. Therefore, based on experimental results, formulae are proposed for the evaluation of the delamination resistance and optimal bonding length, in order to ensure the correct stress transfer that may avoid the premature detachment of the composite from the glass support. These formulae were used to calculate the values of the delamination resistance and the optimal adhesion length in the case of composites in steel-fiber and glass-fiber. The obtained results are in line with experimental ones and in general are greater so these theoretical values will lead to results on the safe side.

REFERENCES

[1] Speranzini E, Agnetti S. The technique of digital image correlation to identify defects in glass structures. Struct Cont and Health Monit 2014; 21: 1015-1029. DOI: 10.1002/stc, 1-15.

[2] Galuppi L, Royer-Carfagni G. The post-breakage response of laminated heat-treated glass under in plane and out of plane loading. Compos Part B Eng. 2014; 64: 202-213.

[3] Foraboschi P. Analytical modeling to predict thermal shock failure and maximum temperature gradients of a glass panel. Mater Design 2017; 134: 301-319. https://doi.org/10.1016/j.matdes.2017.08.021

[4] Castori G, Speranzini E. Structural analysis of failure behavior of laminated glass. Compos Part B Eng 2017; 125: 89-99. https://doi.org/10.1016/j.compositesb.2017.05.062

[5] Speranzini E. & Neri P. On the bending of GFRP Reinforced Glass Elements, In: Proceedings of the International Conference Asia-Pacific Conference on FRP in Structures – HongKong 12-14 December 2007.

[6] Cagnacci E, Orlando M. & Spinelli P. Experimental campaign and numerical simulation of the behavior of reinforced glass beams. In: Proceedings of Glass Performance Days, Tamper, Finland, 12-15 June 2009; pp. 484-487.

[7] Louter C, Belis J, Veer F & Lebet J. Structural response of SG-laminated reinforced glass beams; experimental investigations on the effects of glass type, reinforcement percentage and beam size. Eng Struct 2012; 36: 292-301. https://doi.org/10.1016/j.engstruct.2011.12.016

[8] Nielsen JH. & Olesen JF. Mechanically reinforced glass beams. Struct Eng Mech Comput 2008; 3: 1707-1712.

[9] Bos F.P. 2009. Influence of elastic strain energy release on failure behavior of stainless steel reinforced glass beams. In: Proceedings of Glass Performance Days, Tamper, Finland, 12-15 June 2009: 306-309.

[10] Speranzini E, Agnetti S. "Strengthening of glass beams with steel reinforced polymer (SRP). Compos Part B Eng 2014; 67: 280-289. https://doi.org/10.1016/j.compositesb.2014.06.035

[11] Netusil M, Eliasova M. Design of the composite steel-glass beams with semi-rigid polymer adhesive Joint. J Civil Eng and Architect 2012; 6(57): 1059-1069.

[12] Valarinho L, Correia JR, Branco FA. Experimental study on the flexural behaviour of multi-span transparent glass–GFRP composite beams. Constr Build Mater 2012; 49: 1041-1053. https://doi.org/10.1016/j.conbuildmat.2012.11.024

[13] Speranzini E, Agnetti S. Flexural performance of hybrid beams made of glass and pultruded GFRP. Constr Build Mater 2015; 94: 249-261. https://doi.org/10.1016/j.conbuildmat.2015.06.008

[14] Overend M, Nhamoinesu S, Watson J. Structural performance of bolted connections and adhesively bonded joints in Glass Structures. ASCE J Struct Eng 2012; 139 (12): 04013015. https://doi.org/10.1061/(ASCE)ST.1943-541X.0000748

[15] Adams RD, Wake WC. Structural adhesive joints in engineering. Elsev App Science P. 1984; London and New YorK, USA.

[16] Corradi M, Borri A, Castori G, Speranzini E. Fully reversible reinforcement of softwood beams with unbounded composite plates. Comp Struct 2016; 149: 54-68. https://doi.org/10.1016/j.compstruct.2016.04.014

[17] Cottone A, Giambanco G. Minimum bond length and size effects in FRP-substrate bonded joints. Eng Frac Mech 2009; 76: 1957-76. https://doi.org/10.1016/j.engfracmech.2009.05.007

[18] ASM International. Handbook Committee. Engineered Materials Handbook: Adhesives and Sealants. Vol. 3, CRC, 1990.

[19] Goland M, Reissner E. The Stresses in cemented joints. J ApplMech 1944; 11(1): 11-27.

[20] Corradi M, Borri A, Righetti L, Speranzini E. Uncertainty analysis of FRP reinforced timber beams, Compos Part B Eng 2017; 113: 174-184. https://doi.org/10.1016/j.compositesb.2017.01.030

Received on 22-11-2018 Accepted on 15-12-2018 Published on 31-12-2018

DOI: http://dx.doi.org/10.31875/2409-9848.2018.05.8